

Optical absorption spectra of liquid sulphur over a wide absorption range

This article has been downloaded from IOPscience. Please scroll down to see the full text article.

1994 J. Phys.: Condens. Matter 6 5273

(<http://iopscience.iop.org/0953-8984/6/28/005>)

View [the table of contents for this issue](#), or go to the [journal homepage](#) for more

Download details:

IP Address: 171.66.16.147

The article was downloaded on 12/05/2010 at 18:50

Please note that [terms and conditions apply](#).

Optical absorption spectra of liquid sulphur over a wide absorption range

Shinya Hosokawa[†], Tadashi Matsuoka and Kozaburo Tamura

Faculty of Integrated Arts and Sciences, Hiroshima University, Higashi-Hiroshima 724, Japan

Received 8 February 1994

Abstract. The optical absorption coefficient α of liquid sulphur has been measured in a wide absorption range from 5.5×10^{-2} to $2 \times 10^5 \text{ cm}^{-1}$ at temperatures from 130 to 450 °C. For measurement in the high-absorption range beyond 10^5 cm^{-1} , we have developed an optical cell of our own design with a sample thickness of about 3000 Å. It was found that the absorption spectra are substantially changed at the polymerization temperature, especially in the high-absorption region; a new absorption band appears at around 3.25 eV and increases with increasing temperature. We discuss the origin of this new absorption band in the high-absorption region together with the details of the spectral changes in the intermediate and low-absorption regions.

1. Introduction

Elemental sulphur melts to form a liquid of unique and often striking properties which have attracted considerable attention for many decades [1–3]. Much of the work has focused on the fact that liquid sulphur exhibits a thermodynamic transition between two distinct liquid modifications. Between the melting point (113 °C for orthorhombic sulphur) and the critical polymerization temperature of 159 °C, it forms a light-yellow insulating liquid with a low viscosity consisting of S_8 molecules which have the shape of puckered rings. Above 159 °C, it forms a highly viscous liquid in which a significant fraction of ring molecules polymerize to long polymeric chains containing up to 10^6 atoms. The concentration of chains increases with increasing temperature [4, 5].

Physical properties such as the structure factor [6], magnetic susceptibility [7], ESR [8], density [9], heat capacity [10] and viscosity [11] are influenced by the temperature-dependent structural changes and changes in the molecular composition. A remarkable change in the optical properties also appears; the colour of the liquid changes rapidly from yellow to red with increasing temperature. The optical absorption coefficient has been extensively measured by different investigators [12–16]. Most of the work deals with the temperature dependence of the red shift of the absorption spectra and the influence of the polymerization on the shift rate. In fact, appreciable changes in the electronic states can be expected around the polymerization temperature since the different ring and chain species differ in their structural correlation extending beyond the first neighbours. However, the polymerization seems to have little effect on the optical absorption spectra [13–16] except for the appearance of the low-energy band at around 1.4 eV [15] originating from the diradical chain whose temperature-dependent intensity correlates with the paramagnetism of the chain ends.

[†] Present address: Department of Materials Science, Faculty of Science, Hiroshima University, Higashi-Hiroshima 724, Japan.

Recently, Tamura and co-workers [17] performed a precise measurement of the optical reflectivity in a wide energy region and deduced the absorption spectra from detailed analysis of the reflectivity data. The most surprising feature of the results is the characteristic change in the absorption spectra at about 3.2 eV for temperatures higher than the polymerization temperature of about 160°C which indicates the appearance of a new absorption band. They concluded that the new absorption band is strongly connected with the atoms in the chains.

The main purpose of the present study is to perform a direct measurement of the optical absorption coefficient in a wide absorption range from 5.5×10^{-2} to $2 \times 10^5 \text{ cm}^{-1}$, which may clarify the sensitivity of the optical absorption to the polymerization which has been demonstrated in the optical reflectivity data [17].

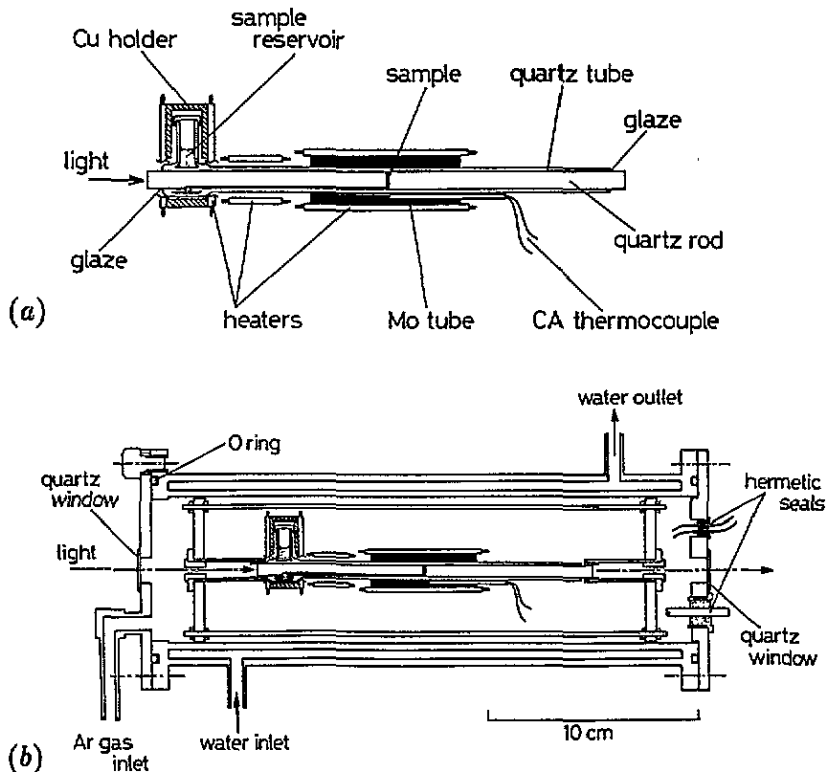


Figure 1. (a) Quartz cell used for the optical absorption measurements: CA, chromel–alumel. (b) Side view of the chamber used for the optical absorption measurements.

2. Experimental details

In order to measure α in the absorption range beyond 10^5 cm^{-1} of liquid sulphur, we had to make an optical cell of our own design with a sample thickness of about 3000 Å, which is illustrated in figure 1(a). Two quartz rods with a diameter of 6.5 mm and a length of 80 mm, the ends of which were polished to have optically flat surfaces, were put in a quartz tube with an inner diameter of 6.5 mm, an outer diameter of 8 mm and a length of 150 mm. The cell had a uniform gap between these two rods in which the liquid sample was located.

As seen in figure 1(a), the sample with a purity of 99.9999% was heated by a heating element made of Mo wire with a diameter of 0.7 mm. In order to reduce the temperature

gradient around the sample, a Mo tube was put between the cell and the heater. The temperature was measured by two chromel–alumel thermocouples attached on the outside wall of the cell through the holes drilled in the Mo tube. The sample reservoir was encased in a Cu holder which trapped sulphur vapour escaping from the reservoir. Another heating element made of Mo wire with a diameter of 0.5 mm was put around the Cu holder to keep the temperature of the reservoir at about 150°C.

The optical cell was positioned in a cylindrical water-cooled chamber with two windows made of quartz, the side view of which is illustrated in figure 1(b). As shown in the figure, the light passed through the quartz windows, the quartz rods and the liquid sulphur. The electrodes for the heaters and the thermocouples were taken into the chamber through hermetic seals. The chamber was fixed on x - and z -translational stages adjustable to the light path.

The sample space of the cell was filled with liquid sulphur in the following way. First, the chamber was evacuated and the sample space was heated to 150°C. Then, the solid sulphur loaded in the reservoir was melted by heating it to 150°C. Finally, Ar gas at atmospheric pressure was introduced into the chamber to force the liquid sulphur into the sample space through a narrow channel between the quartz rod and the tube.

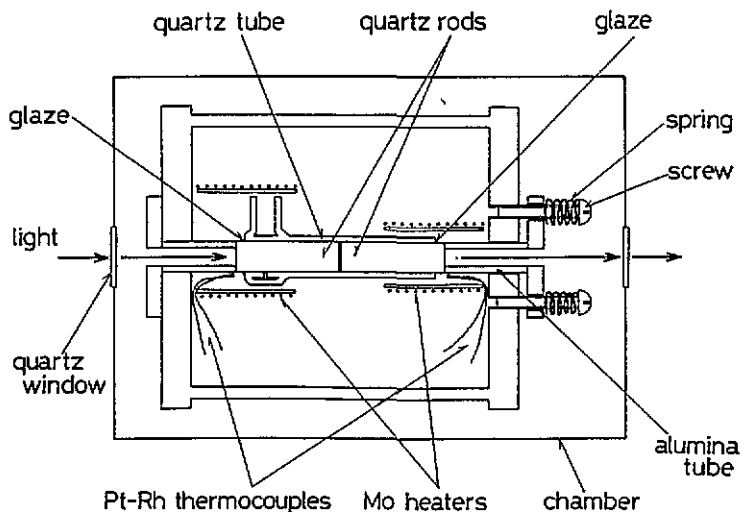


Figure 2. Schematic view of the chamber used for the construction of the optical cell.

Here, we should note that it is extremely difficult to construct the optical cell keeping such a liquid thin film, especially with a high vapour pressure, stable. So we briefly describe the method of how to make it. Figure 2 shows a schematic view of a chamber used to construct the quartz cell. The vertical scale is enlarged so that it is easy to see. First, a small amount of fine graphite powder was put into the space between the rods. Then, the rods were pushed by two alumina tubes, making a very small gap between rods, in the chamber. The alumina tube on the right-hand side was supported by the springs. If the gap was not uniform, many interference fringes were observed on illumination by the yellow light of an Na lamp. When these interference fringes disappeared by adjusting the strength of the spring, a uniform gap had been obtained. Then, we pasted a high-temperature glaze (Vitta type P-1015) at the positions shown in the figure and cemented by the cell by heating it to 950°C in Ar gas. Finally, the graphite powder was completely burnt out in the air

by heating the cell to 550°C. The thickness of the gap or the optical path length was determined again by the optical interference method. We have previously measured α for liquid Se [18], As₂S₃ and As₂Se₃ [19] using the same type of the cell.

We measured α using a Jasco CT-25GD spectrometer in the wide photon wavelength range from 260 to 2500 nm, which corresponds to the energy range from about 0.50 to 4.75 eV. In order to obtain α from the measured optical transmittance, we took account of various corrections, of which the following four were very important: optical reflectance, interference fringes, temperature variations in the sample thickness and temperature variations in the optical absorption of the quartz cell.

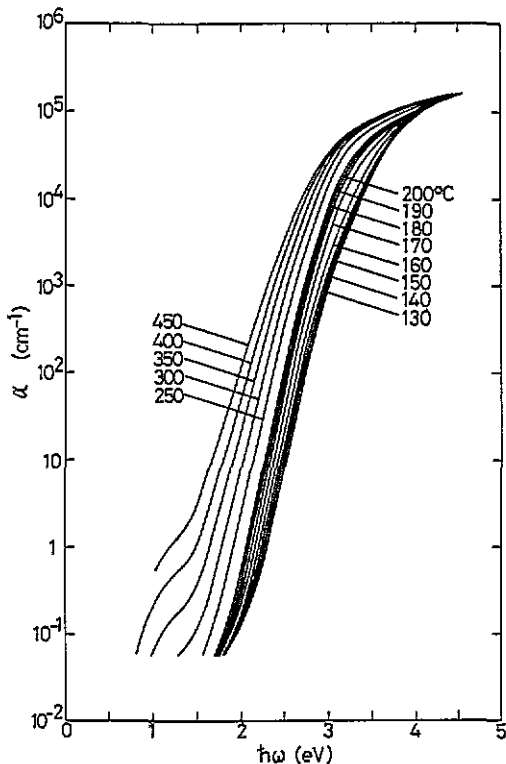


Figure 3. Logarithmic plots of the optical absorption coefficient α for liquid sulphur as a function of photon energy $\hbar\omega$ at various temperatures.

3. Results

Figure 3 shows the logarithmic plots of α for liquid sulphur as a function of photon energy. The spectra are shown at temperatures every 10°C from melting point to 200°C and every 50°C in the higher-temperature range. The spectra at 450°C were measured at slightly higher pressure than atmospheric pressure. For the measurements we used optical cells with different optical path lengths of about 40 mm, 4 mm, 0.5 mm, 40 μm , 1.8 μm , 0.5 μm and 0.3 μm , which enabled us to measure α in the range from 5.5×10^{-2} to $2 \times 10^5 \text{ cm}^{-1}$. It should be noted that this is the first measurement of α in a very wide absorption range of more than six orders of magnitude including the high-absorption range exceeding 10^5 cm^{-1} . Our results are in good agreement with the previous data [14–16] in the absorption range around 10 cm^{-1} , but less consistent in the lower-absorption region.

As seen in the figure, there is a substantial red shift of the spectrum with increasing temperature. The absorption curves seem to be decomposed into three parts as observed in

amorphous semiconductors: the high-absorption part with a power dependence on photon energy, the intermediate part with an exponential variation, and a weak shoulder in the low-absorption region. It should be noted that in the high-absorption region a new absorption band appears at around 3.25 eV accompanied by polymerization at 160 °C, which increases rapidly with increasing temperature. The slope of the exponential tail in the intermediate-absorption region decreases with increasing temperature. In the low-absorption region, an absorption band appears at around 1.3 eV at temperatures higher than about 300 °C, which increases with increasing temperature.

4. Discussion

The characteristic yellow colour of liquid sulphur below the polymerization temperature originates from the optical absorption clearly demonstrated by the absorption curve in figure 3, which corresponds to the long-wavelength tail of an intrinsic absorption band peaking at about 4 eV. The 4 eV band has been attributed to the lone-pair (LP) states $\rightarrow \sigma^*$ (antibonding states) transition [20]. This assignment is based on the molecular orbital analysis and tight-binding ideas [21, 22] for the isolated S_8 -ring molecule. The chalcogens have an s^2p^4 valence configuration; two of the p orbitals form σ bonds, leaving s and LP orbitals. The LP states lie at the top of the valence band and σ^* states form the conduction band. In the low-temperature liquid, the weak van der Waals interaction between ring molecules broadens the energy levels of the isolated S_8 rings only slightly [23]. However, the assignment to the LP $\rightarrow \sigma^*$ transition is not fully supported by another molecular orbital calculation [24, 25]. When electron–electron interactions are included, the description in terms of one-electron levels no longer suffices. The molecular orbital calculation [24, 25] indicates that in the S_8 -ring molecule the energy interval between the highest filled and lowest empty levels is found to be about 9 eV. Therefore the absorption band of the S_8 ring located at around 4 eV may be dominated by exciton creation processes [24] which is supported by photogeneration studies [26].

It is obvious from figure 3 that the polymerization transition changes the absorption spectrum especially in the high-absorption range, to which the rapid colour change of liquid sulphur above the polymerization temperature is attributed. We discuss now the details of spectral changes in the three different absorption regions as follows.

4.1. High-absorption region

The temperature variation in absorption spectra in the high-absorption region, i.e. beyond 10^4 cm^{-1} , is marked at around the photon energy of 3.25 eV. Figure 4(a) shows linear plots of α at a photon energy of 3.25 eV as a function of temperature. At temperatures below the polymerization temperature, α at 3.25 eV slightly and almost linearly increases with increasing temperature, while an abrupt increase is observed immediately above the polymerization temperature. At temperatures above 300 °C, the increase in α at 3.25 eV becomes relatively small. Such a variation in α with temperature is quite similar to that of the absorption spectra computed from the reflectivity data using a classical-oscillator-fit analysis [17]. Further, absolute values of α at 3.25 eV in the literature [17] are almost the same as those of the present measurement, which suggests that their classical-oscillator-fit analysis is quite reasonable to extract the correct absorption spectrum from the reflectivity data.

It should be noted that the increase in α with increasing temperature as shown in figure 4(a) is very similar to the increase in the concentration of chains reported by Koh

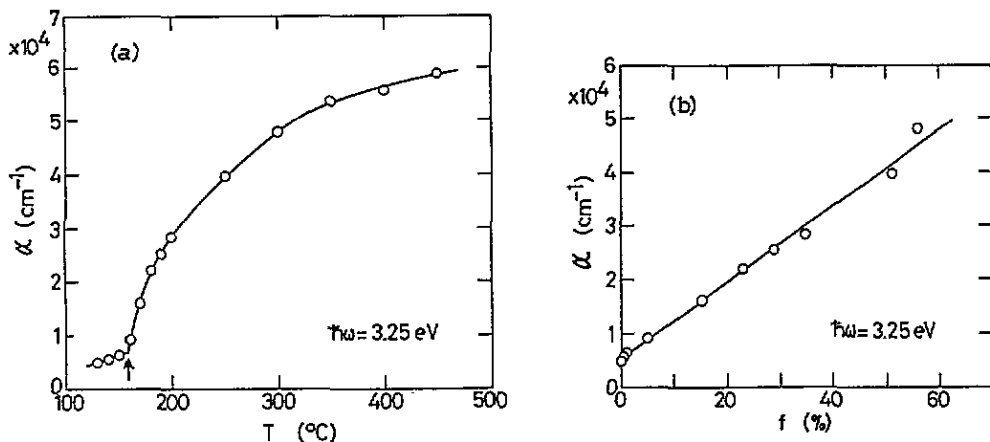


Figure 4. Linear plots of α at a photon energy of 3.25 eV as functions of (a) temperature and (b) the concentration f of atoms in chain obtained by Koh and Klement [5]. The arrow indicates the polymerization temperature. The solid lines are guides for the eye.

and Klement [5]. Figure 4(b) shows α at 3.25 eV as a function of the concentration f of atoms in the chain [5]. We find a strong correlation between α and f . Thus, the equivalence of these temperature dependences is strong evidence that the optical absorption at 3.25 eV is closely connected to the atoms in chains. This result is in contrast with the conclusion drawn from a comparison [14] of earlier measurements of the low-energy part of the absorption edge and preliminary calculations of the energy levels of ring and chain that the polymerization does not affect the electronic levels. Our result is in agreement with an unpublished preliminary calculation by Salaneck [27]. He made a comparison of electronic levels between an S_8 ring and an S_9 chain assuming that they had the same bond angles and lengths. He found that the first optical absorption is 0.2 eV lower for the S_9 chain than the S_8 ring. It is reasonable to assume that in the very long chains of sulphur atoms, which appear immediately above the polymerization temperature, the first optical absorption moves to still lower energies owing to delocalization of the wavefunctions. In fact, the most recent calculation for the infinite linear chain of sulphur [28] gives a small band-gap energy of about 2 eV for an infinite helical chain of sulphur.

As is well known, the absorption spectrum in the high-absorption region is closely connected to the electronic transition from the valence to conduction band. From the detailed analysis of the spectra, we obtain the optical gap E_g , defined by the conventional relation $(\alpha\hbar\omega)^n \propto \hbar\omega - E_g$, where n is a constant [29]. Figures 5(a), 5(b) and 5(c) show the plots of $(\alpha\hbar\omega)^n$ versus $\hbar\omega$ at 150°C below the polymerization temperature assuming the values of n to be $\frac{1}{2}$, 1 and $\frac{3}{2}$, respectively. As is well known, the values of n are taken to be $\frac{1}{2}$ for most amorphous semiconductors. For amorphous Se we take it to be 1, which is attributed to the sharp rise at the edges of the density of states, and strongly connected with the one-dimensional character of the chain structure of amorphous Se [30]. As clearly seen in the figure, the plots lie on the straight line when $n = \frac{3}{2}$. Note that $\frac{3}{2}$ is the largest value of n for many amorphous [29] and liquid [18, 19] semiconductors, which may be related to the zero-dimensional character of the weakly interacting S_8 ring molecules in liquid below the polymerization temperature. The value of E_g for liquid sulphur at 150°C is 3.65 eV and decreases slightly with increasing temperature. The value of E_g of the orthorhombic sulphur consisting of S_8 ring molecules is 3.45 eV [31].

At temperatures higher than the polymerization temperature, we found that the plots of α could not lie on one straight line for any selected values of n , which may be caused by

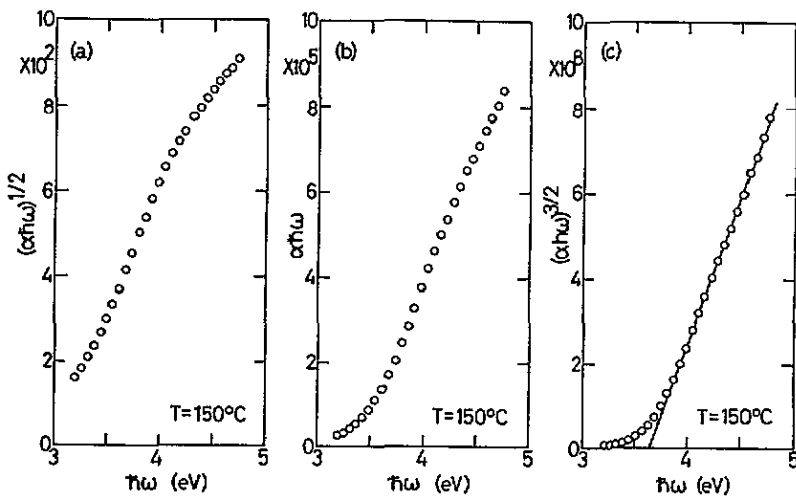


Figure 5. Plots of $(\alpha\hbar\omega)^n$ versus $\hbar\omega$ at 150°C below the polymerization temperature assuming the value of n to be (a) $\frac{1}{2}$, (b) 1 and (c) $\frac{3}{2}$.

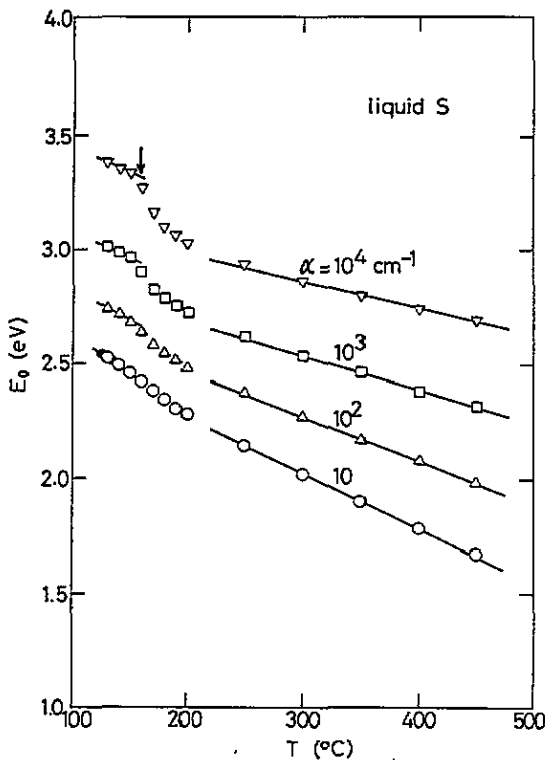


Figure 6. Photon energies at which $\alpha = 10 \text{ cm}^{-1}$ (O), 10^2 cm^{-1} (Δ), 10^3 cm^{-1} (\square) and 10^4 cm^{-1} (∇) as functions of temperature: \bullet , photon energy at which $\alpha = 10 \text{ cm}^{-1}$ obtained by Donaldson and Caplin [16]. The arrow indicates the polymerization temperature.

the fact that there is a mixing of rings and chains in the liquid above the polymerization temperature.

4.2. Intermediate-absorption region

Previous measurements of α were limited in the intermediate region from 1 to 10^3 cm^{-1} . Most of the work has focused on the temperature variation in the red shift of the absorption

spectra and the influence of the polymerization on the shift rate. Zanini and Tauc [14], Weser *et al* [15] and Donaldson and Caplin [16] investigated the temperature dependence of the energy E_0 at which α has a constant value and pointed out that no discontinuous behaviour in the temperature dependence of E_0 was observed. These observations have led to the incorrect conclusion that the polymerization has little effect on the electronic states. Meyer *et al* [12], on the contrary, obtained the completely opposite result that the rate of the red shift with temperature shows a clear change at the polymerization temperature. In order to give a clear solution to the controversy, we plot E_0 versus temperature for different values of α as shown in figure 6. Open circles, open triangles, open squares and open inverted triangles indicate E_0 for which $\alpha = 10 \text{ cm}^{-1}$, 10^2 cm^{-1} , 10^3 cm^{-1} and 10^4 cm^{-1} , respectively. Note that E_0 at which $\alpha = 10^3\text{--}10^4 \text{ cm}^{-1}$ is well known to be a conventionally defined optical gap. For the case when $\alpha = 10 \text{ cm}^{-1}$, E_0 decreases continuously with increasing temperature and no anomalous behaviour is found at the polymerization temperature which has been certainly observed in previous research [14–16] while, for $\alpha = 10^2$, 10^3 and 10^4 cm^{-1} , E_0 markedly decreases around the polymerization temperature.

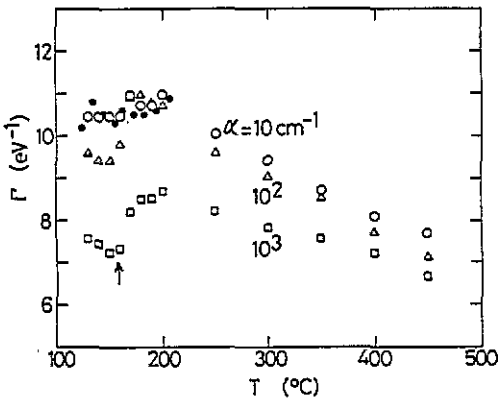


Figure 7. Slope of the Urbach tail Γ at which $\alpha = 10 \text{ cm}^{-1}$ (O), 10^2 cm^{-1} (Δ) and 10^3 cm^{-1} (\square) as functions of temperature: \bullet , Γ at $\alpha = 10 \text{ cm}^{-1}$ obtained by Donaldson and Caplin [16]. The arrow indicates the polymerization temperature.

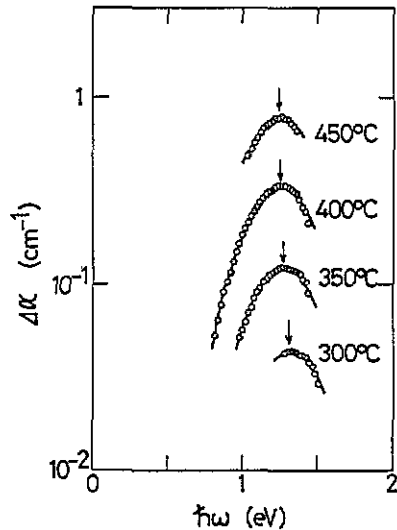


Figure 8. Plots of the absorption coefficient $\Delta\alpha$ obtained by subtracting the exponentially varying Urbach tail.

As seen in figure 3, each spectra shows an exponential dependence on energy, given by $\alpha = C \exp(\Gamma\hbar\omega)$, which is called an Urbach tail, where Γ is the slope of the exponential tail and C a constant. It should be noted that the spectra do not exactly lie on the straight lines and are slightly bent. The values of Γ at the photon energy at which α becomes 10, 10^2 and 10^3 cm^{-1} are plotted in figure 7 as a function of temperature. Open circles, open triangles and open squares indicate Γ at $\alpha = 10 \text{ cm}^{-1}$, 10^2 cm^{-1} and 10^3 cm^{-1} , respectively. Full circles indicate Γ at $\alpha = 10 \text{ cm}^{-1}$ obtained by Donaldson and Caplin [16]. As they pointed out in their paper, the temperature variation in Γ at $\alpha = 10 \text{ cm}^{-1}$ shows no evidence of the polymerization transition. Note that, however, those of Γ at $\alpha = 10^2$ and 10^3 cm^{-1} again show substantial jumps at the polymerization temperature.

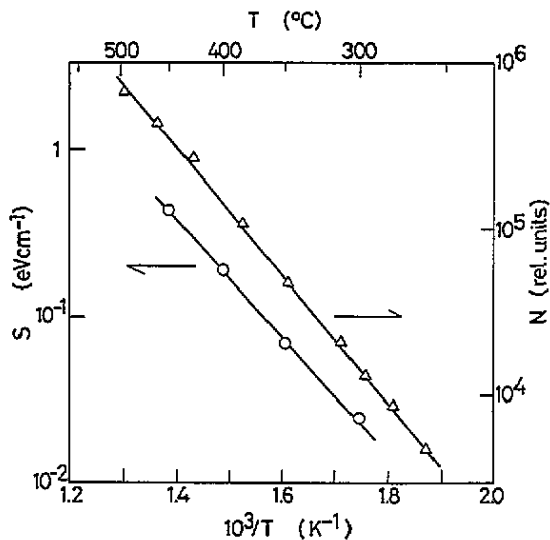


Figure 9. Logarithmic plots of the area of the absorption band appearing in the low-absorption region as a function of reciprocal temperature together with the magnitude of the ESR signal [8].

4.3. Low-absorption region

In the low-absorption region, i.e. below about 1 cm^{-1} , a new absorption band appears at about 300°C around 1.3 eV and increases rapidly with increasing temperature. This band was found for the first time by Weser *et al* [15]. From the comparison of the area of their absorption band with the magnitude of the ESR signal [8], they concluded that the band originated from the dangling bond at the sulphur chain ends. We have also studied the absorption band. Figure 8 shows the plots of the absorption coefficient $\Delta\alpha$ obtained by subtracting the exponentially varying Urbach tail. It is obvious that the logarithmic plots of $\Delta\alpha$ lie on the parabolic curves indicated by the solid lines. With increasing temperature the band increases and the maximum position at around 1.3 eV at 300°C shifts to a lower energy. Figure 9 shows plots of the logarithm of the area of the absorption band as a function of reciprocal temperature which are indicated by open circles. These open circles lie on a straight line. The activation energy estimated from the slope is 0.70 eV , which is slightly smaller than the value of 0.82 eV obtained from the ESR measurements. For comparison, the temperature variation in ESR signal is also plotted in figure 9. The similarity of these temperature dependences is strong evidence that the optical absorption at around 1.3 eV is connected with the dangling bonds of the chain, which has been experimentally pointed out by Weser *et al* [15] and theoretically predicted by Salaneck [27].

5. Summary

We have measured α for liquid sulphur in a wide absorption range from 5.5×10^{-2} to $2 \times 10^5 \text{ cm}^{-1}$. For measurements in the high-absorption range, we have developed a quartz cell of our own design with a sample thickness of 3000 \AA . It was found that the higher-order structural change accompanied by the polymerization transition affects substantially the optical absorption spectra in the high-absorption region; a new absorption band appears at around 3.25 eV at the polymerization temperature and increases with increasing temperature. This new absorption band is closely connected to the electronic states of the polymeric chains. An Urbach tail is observed in the intermediate-absorption range from 1 to 10^4 cm^{-1} . The temperature variation in the slope of the tail shows a distinct jump at the polymerization temperature in the absorption range beyond 10^2 cm^{-1} . In the low-absorption region, the

absorption band originating from dangling bonds of the chains appears at temperature above 300 °C and increases with increasing temperature.

Acknowledgments

The authors are grateful to Professor F Hensel, Professor M Watabe and Professor K Hoshino for helpful discussions in the present study. This work was partly supported by a Grant-in-Aid for Scientific Research from the Ministry of Education, Science and Culture of Japan.

References

- [1] Steudel R 1982 *Top. Curr. Chem.* **102** 149
- [2] Meyer B 1976 *Chem. Rev.* **76** 367
- [3] Schmidt M 1973 *Angew. Chem.* **85** 474
- [4] Mäusele A J and Steudel R 1981 *Z. Anorg. (Allg.) Chem.* **478** 177
- [5] Koh J C and Klement W Jr 1970 *J. Phys. Chem.* **74** 4280
- [6] Tompson C W and Gingrich N S 1959 *J. Chem. Phys.* **31** 1598
Winter R, Bodensteiner T, Szornel C and Egelstaff P A 1988 *Non-Cryst. Solids* **106** 100
Winter R, Szornel C, Pilgrim W-C, Howells W S, Egelstaff P A and Bodensteiner T J 1990 *J. Phys.: Condens. Matter* **2** 8427
- [7] Poulis J A, Massen C H and van der Leeden P 1962 *Trans. Faraday Soc.* **58** 474
- [8] Koningsberger D C and de Neets T 1990 *Chem. Phys. Lett.* **4** 615; 1972 *Chem. Phys. Lett.* **14** 453
- [9] Kellas A M 1918 *J. Chem. Soc.* **113** 903
- [10] West E D 1959 *J. Am. Chem. Soc.* **81** 29
- [11] Schenk J 1957 *Physica* **23** 325
- [12] Meyer B, Oommen T V and Jensen D 1971 *J. Phys. Chem.* **75** 912
- [13] Bröllös K and Schneider G M 1972 *Ber. Bunsenges. Phys. Chem.* **76** 1106; 1974 *Ber. Bunsenges. Phys. Chem.* **78** 296
- [14] Zanini M and Tauc J 1977 *J. Non-Cryst. Solids* **23** 349
- [15] Weser G, Hensel F and Warren W W Jr 1978 *Ber. Bunsenges. Phys. Chem.* **82** 588
- [16] Donaldson A and Caplin A D 1985 *Phil. Mag.* **B 52** 185
- [17] Tamura K and Hensel F 1983 *J. Non-Cryst. Solids* **59–60** 1079
Tamura K, Seyer H-P and Hensel F 1986 *Ber. Bunsenges. Phys. Chem.* **90** 581
- [18] Hosokawa S and Tamura K 1990 *J. Non-Cryst. Solids* **117–118** 489
- [19] Hosokawa S, Sakaguchi Y, Hiasa H and Tamura K 1991 *J. Phys.: Condens. Matter* **3** 6673
- [20] Cook B E and Spear W E 1969 *J. Phys. Chem. Solids* **30** 1125
- [21] Gibbons D J 1970 *Mol. Cryst. Liq. Cryst.* **10** 137
- [22] Chen I 1970 *Phys. Rev. B* **2** 1053
- [23] Salaneck W R, Lipari N O, Paton A, Zallen R and Liang K S 1975 *Phys. Rev. B* **12** 1493
- [24] Emerald R L, Drews R E and Zallen R 1976 *Phys. Rev. B* **14** 808
- [25] Salaneck W R, Duke C B, Paton A, Griffiths C and Keezer R C 1977 *Phys. Rev. B* **15** 1100
- [26] Mizobuchi Y, Kato H, Shintani R and Ooshita Y 1971 *J. Phys. Soc. Japan* **31** 155
- [27] Salaneck W R 1977 private communication
- [28] Springborg M and Jones R O 1986 *Phys. Rev. Lett.* **57** 1145
- [29] See, e.g., Mott N F and Davis E A 1979 *Electronic Processes in Non-crystalline Materials* (Oxford: Clarendon) p 273
- [30] Mott N F and Davis E A 1979 *Electronic Processes in Non-crystalline Materials* (Oxford: Clarendon) p 523
- [31] Spear W E and Adams A R 1966 *J. Phys. Chem. Solids* **27** 281
Rathenau G 1936 *Physica* **3** 42